A five-dimensional quantum mechanical study of the H+CH$_4$→H$_2$+CH$_3$ reaction

Henrik Szichman[a)] and Roi Baer[b)]
Institute of Chemistry and Lise Meitner Center for Quantum Chemistry,
The Hebrew University of Jerusalem, Jerusalem 91904, Israel

A quantum mechanical approach to the treatment of atom–penta-atom abstraction process of the type E+FABCD→EF+ABCD is presented. The initial 12 degrees of freedom problem is simplified to a reaction having only 7 active degrees of freedom, emulating a rotating–stretching FABCD molecule. Its internal angles are frozen at their equilibrium values as the molecule collides with an attacking E atom. This model is then applied to the study of the H+CH$_4$→H$_2$+CH$_3$ reaction, predicting for the first time remarkable non-Arrhenius behavior. The dynamics was based on the Jordan and Gilbert analytical potential energy surface (JG-PES). The method employs the infinite-order-sudden-approximation (IOSA) method for the methane (CH$_4$) rotations. Next, the coupled states (CS or j_z) approximation is used to decouple the total angular momentum **J** from internal rotational operators. Finally, precessions are overcome by averaging the JG-PES around the out-of-plane angle in the attacking atom geometry. This treatment leads to a five-dimensional fully quantum mechanical computation for determining the total reaction probabilities, cross sections, and temperature-dependent rate constants. Comparing with experiment, the calculated rate constants show good agreement at high temperatures. At lower temperatures there are pronounced tunneling effects. A detailed comparison is made to other theoretical and experimental treatments. © *2002 American Institute of Physics.* [DOI: 10.1063/1.1508372]

I. INTRODUCTION

Understanding the fundamentals of combustion processes is important for scientific, economical, and ecological reasons. The challenge for experimental and theoretical chemistry is substantial, and requires a combined effort of the two disciplines. For a fruitful interplay between theory and experiment, a benchmark system must be adopted, on which calculations and empirical data can be compared. The H+CH$_4$→H$_2$+CH$_3$ reaction is emerging as such a system to study fundamental hydrogen abstraction processes creating methyl radicals. Indeed, a large body of investigations, both experimental[1–14] and theoretical,[15–26] have emerged during the past years. Typically for combustion reactions, this molecule is suspect of an important role to quantum effects, being composed particularly of hydrogen.

The reaction H+CH$_4$→H$_2$+CH$_3$ has been extensively studied experimentally in the 424–1600 K range. Thermal rate constants have been reported by a large number of investigators.[1–14] A comparison of the different experimental data revealed striking differences on the estimation of the activation energy (from 15.1–11.5 kcal mole^{-1} evaluated at high temperature ranges[2,3,8] to 8–4 kcal mole^{-1} obtained at low ranges[1,14]). These deviations from the Arrhenius behavior cannot be explained on the basis of any known classical theory. Using transition state (TS) phenomenological modeling, Clark and Dove[6] first, and later corroborated by Tsang and Hampson,[12] found a best fit to experimental data using a

temperature-dependent A factor of T^3 in the Arrhenius formula. Summarizing, the experimental evidence suggests that the present reaction may be highly influenced by quantum effects such as tunneling phenomena.

The effective interplay of experiment and theory relies to a large extent on the availability of a high quality *ab initio* potential energy surface (PES). Jordan and Gilbert[15] developed a new PES, the JG-PES, based essentially on functional forms employed by Joseph *et al.*[16] The difference exists in the fact that the four H's of methane are treated symmetrically in Ref. 15, even though that some evidence contradicting this claim has been published.[17] A well-known qualitative feature of this reaction, drawn from previous PES[18–20] is that the transition state has a ''collinear'' H+H–CH$_3$ structure following closely a C_{3V} symmetry throughout the process. This feature is preserved also in the JG-PES. While this feature is similar to previous work, it is to be expected that the JG-PES has a more accurate reaction barrier height and structure.

The collinear nature of the transition state served as a base for several three-dimensional (3-D) and four-dimensional (4-D) quantum mechanical (QM) calculations. Takayanagi[21] treated the system as a linear four-atom chemical reaction, treating three dimensions, finding too high rate constants, compared to experiment, attributed to tunneling effects. However, they did not observe a significant departure from Arrhenius behavior. In the second, Yu and Nyman[22] employed a rotating bond umbrella (RBU) model in which the reagent CH$_4$ is treated as a pseudolinear triatomic molecule, including a bending mode to obtain a 4-D model. This

calculation predicted still higher rate constants with lower activation energy and no deviance from Arrhenius behavior. Recently, Zhang and co-workers applied their 4-D semirigid vibrating rotor target (SVRT) model with similar purposes, considering the CH_4–methane molecule globally within an optimized geometry.[23] This study showed markedly lower reaction rates and a higher activation energy than the previous theoretical studies. The variational transition state theory with semiclassical tunneling corrections was also used for studying this system.[24] The results of that application showed large deviations from experiment at high temperatures. At lower temperatures, the deviation from Arrhenius behavior qualitatively similar to experimental results was reported. Recently, a fully dimensional method was used[25] to obtain the rate constant for $J=0$. The results cannot be directly compared to experiment because they are relevant only for very low temperatures. Recently an attempt to improve this method was published.[26]

In this paper we study the benchmark reaction $H+CH_4 \rightarrow H_2+CH_3$ using a high-dimensional quantum method. Previous QM theoretical calculations have not reported a significant deviation from Arrhenius behavior for this reaction.[21–23,25] The specific question we seek to answer is whether this observation is a result of the JG-PES or from reduced dimensional calculations. To answer such a question, a high-dimensional quantum calculation is required. Thus, we present here a quantum mechanical method for calculating reaction probabilities in polyatomic molecular encounters. The method relies on a recently published four-dimensional infinite-order-sudden-approximation (IOSA) quantum mechanical (QM) methodology that was used to study the penta-atomic system HC_2H_2.[27,28] The approach is essentially an extension to higher dimensions of 3-D schemes that had been applied in the past to the study of the dynamics of three- and four-atom molecules.[29–35] An attractive feature of the method is that only nonreactive probabilities in the reagents arrangement channel (AC) need to be calculated. The total reaction probability is then obtained by subtracting their sum from unity.[27,29–32,34,36] This avoids the coordinate transformations to reactive AC's, decreasing considerably the complexity and computational load of the calculation. This procedure also reduces error propagation arising from the multiple use of decoupling schemes of different momenta, such as, for example, the coupled-state (CS or j_z) approximation.[37] Since a reliable symmetrized analytic expression for the six-atom system HCH_4 PES became available[15] not long ago, it is only natural to extend similar calculations to these higher-dimensional molecular systems.

In order to apply the method to the atom–penta-atom reaction, various important changes, with respect to the diatom–diatom system treated previously were required: (a) the mathematical radial analysis is increased to five dimensions; (b) the CH_4 system is now characterized by an atom–diatom recursive linkage rather than by a diatom–diatom configuration of Refs. 27 and 28 for the C_2H_2 molecule; and (c) the hexa-atomic molecule CH_5 is geometrically described by a trihedral surface. To fully describe this PES in all of its internal degrees of freedom, it is necessary to use two independent spatial coordinates systems and a 3-D rotational transformation to relate to both systems.

Our main conclusion in the paper, beside the presentation of the method, is that high-dimensional treatment of the system can lead to significant deviance from Arrhenius behavior, consistent with experimental results. One possibility for the missing effect from previous studies is that reduced dimensionality methods may miss tunneling effects that are due to narrow restrictions in the transverse directions. The paper is organized as follows. In Secs. II–IV, we review the theoretical QM method employed in this research. The results and discussion are provided in Sec. V, and Sec. VI is for the summary and final comments.

II. SIX-ATOM REACTIVE SCATTERING THEORY

A. Arrangement decoupling scattering approach

The theory, upon which the present approach is based, is not different from that already published for tri-, tetra-, and penta-atom systems,[27,29–32,34,36] (which in practice is valid for any polyatomic system). We consider the total Hamiltonian H of the system,

$$H = T + U, \tag{1}$$

composed of a kinetic energy of all the nuclei T and a potential energy term U describing the interaction, within the Born–Oppenheimer approximation, between these particles. In our system, U is the JG-PES, of which more will be said later. In order to describe the initial scattering state, coming from the λ (reagents) arrangement channel (AC), we define the reactants Hamiltonian:

$$H_\lambda = H - V_r, \tag{2}$$

which governs the dynamics of the system before the collision. The potential V_r is localized in the reaction zone and describes the coupling of the reagents AC to the reactive ACs. While we aim at reaction probabilities, the benefit of our approach is that it is performed primarily in the nonreactive channel. For this channel we obtain the scattering S-matrix and transition T-matrix elements, and[38]

$$T(t_{f\lambda} \leftarrow t_{i\lambda}) = \delta_{t_{f\lambda}t_{i\lambda}} - S(t_{f\lambda} \leftarrow t_{i\lambda}), \tag{3}$$

$$S(t_{f\lambda} \leftarrow t_{i\lambda}) = \frac{1}{i\hbar} \langle \psi_{t_{f\lambda}} | V_r | \psi_{t_{i\lambda}} \rangle. \tag{4}$$

From these the total reaction probability can be computed, and many parameters of interest, e.g., integral probabilities, cross sections, opacity-J distributions, and finally rate constants, may then be obtained via the T-matrix elements by means of standard formulas.[27,29–32,34] In these equations, $t_{i\lambda}$ represents the set of quantum numbers describing the initial state $\psi_{t_{i\lambda}}$ in the λ AC (the symbol $\delta_{t_{f\lambda},t_{i\lambda}}$ is the Kronecker delta function). The initial and final states $\psi_{t_{i\lambda}} \psi_{t_{f\lambda}}$ are eigenstates of the asymptotic reagents AC Hamiltonian H_λ. Thus,

$$(E - H_\lambda)\psi_{t_{i\lambda}} = 0. \tag{5}$$

Let the state Ψ_λ represent the part of the total scattering wave function that is in the reaction region and reflected

back into the λ arrangement channel. From this state one can project out the relevant $\psi_{t_{f\lambda}}$. In principle, Ψ_λ is an eigenstate of the total Hamiltonian H corresponding to the given initial state. It is split into two parts,

$$\Psi_\lambda = \psi_{t_{i\lambda}} + \chi_\lambda. \tag{6}$$

The so-called perturbed wave functions χ_λ is obtained by solving the following inhomogeneous SE in the close-interaction region:

$$(E - H_I)\chi_\lambda = V_r \psi_{t_{i\lambda}}, \tag{7}$$

where $H_I = H + V_I$ contains the negative imaginary potentials (NIPs),[39] V_I, which supply the necessary absorbing boundary conditions, eliminating the need to consider fully the reactive channels. Projection methods can be used to extract more specific data from the perturbed wave function in the reagents AC.

B. Kinematics

The method outlined in Sec. II A relies on an efficient representation of the nuclear configuration of the reagents. Because it is not required to fully describe the asymptotic products ACs, it is sufficient to use a coordinate system optimized for the reagents. In particular, a method that elegantly handles the CH_3 symmetry is warranted. We use a set of generalized Jacobi coordinates, that are generated by a recursive atom–diatom configuration[40] similar to the Jepsen and Hirschfelder "mobile" model[41] for a six-atom molecule. Our application of the "mobile" model idea incorporates also out-of-plane motion using orbital angles. The use of these warrants inclusion of body-frame (BF) and fixed-space components into the canonical Hamiltonian according to the principles of classical mechanics. Because the JG-PES of the system is given in terms of the Cartesian coordinates of the nuclei, we were led to combine the Jacobi radial coordinates with orbital angles. This method of specifying the configuration of the system is shown in Fig. 1. (*Note*: since the entire process is described in the reagents AC only, the subscript λ is omitted from the variables shown in the figure.)

The original atom–diatom BCD linkage of Ref. 40 is extended to a general atom–polyatom scheme. Each new atom joining the system is connected through a radial distance ρ to the center of mass of all the atoms already present. In this manner, five radial distances are created, as shown in Fig. 1: four stretches r, ρ_2, ρ_1, ρ, and a translational distance R connecting the attacking atom E (here, the hydrogen nucleus) to the center of mass of the penta-atom FABCD (the methane molecule in our case).

Seven orbital angles then complete the description of the system, where four of them are the polar angles: θ_2, θ_1, θ, and γ (the angles sustained, respectively, between r and ρ_2;
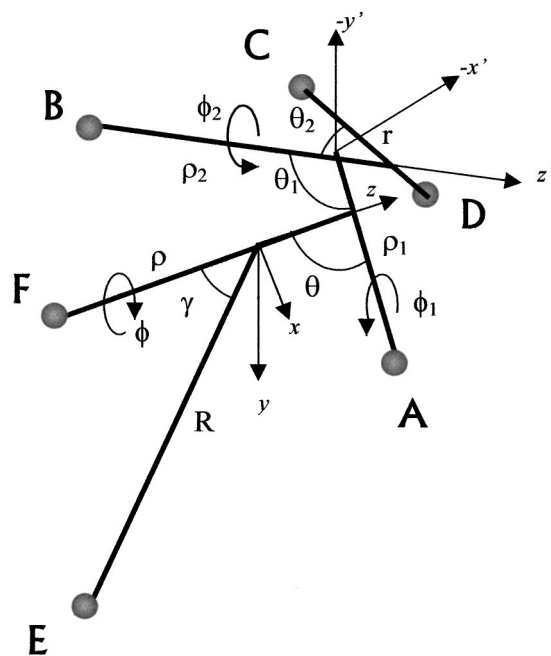

FIG. 1. The 12 generalized Jacobi coordinates for the six-atom (reagents) AC studied in the present work. Note that (1) the $\mathbf{x}'$ and $\mathbf{y}'$ abscissas are indicated in the reverse direction: (2) the azimuthal loops indicate rotations from 0° to 180°.

ρ_2 and ρ_1; ρ_1 and ρ and R). The three azimuthal angles ϕ, ϕ_1, and ϕ_2 then describe as rotations of R around ρ, ρ_2 around ρ_1, and r around ρ_2, as indicated in Fig. 1.

These coordinates describe the internal configuration of the molecule. The position in space of each nucleus (Fig. 1) is given with respect to a certain arbitrary Cartesian frame of coordinates, designated as $S\{x,y,z\}$. The origin of $S\{x,y,z\}$ was chosen at the center of mass of the FABCD molecule (methane in the present case). The $\mathbf{z}$ axis follows the $\boldsymbol{\rho}$ direction and the $(\mathbf{z},\mathbf{x})$ plane is identical to the $(\boldsymbol{\rho},\boldsymbol{\rho}_1)$ plane. $S\{x,y,z\}$ can be straightforwardly used to describe the coordinates of nuclei A, E, and F. In order to facilitate the description of nuclei B, C, and D, it is convenient now to define a secondary frame of reference $S'\{x',y',z'\}$ located at the center of mass of the triatom BCD, where the $\mathbf{z}'$ axis is parallel to the $\boldsymbol{\rho}_2$ direction and the $(\mathbf{z}',\mathbf{x}')$ plane is defined as the $(\boldsymbol{\rho}_2,\boldsymbol{\rho}_1)$ one. By means of trigonometric relations and a spatial rotation transformation, divided into three elementary planar rotations,[42] the space coordinates of the atoms of B, C, and D in S' can be related to S:

$$\mathfrak{R}(S \leftarrow S') = \mathfrak{R}_{z,x}(\theta_1) \times \mathfrak{R}_{x,y}(\phi_1) \times \mathfrak{R}_{z,x}(\theta), \tag{8}$$

where, for example, $\mathfrak{R}_{z,x}(\theta_1)$ denotes an elementary rotation operator in the $(\mathbf{z},\mathbf{x})$ plane through the angle θ_1, and so on as well as for the other operators in Eq. (8). The last equation has been developed into the following expression:

$$\mathfrak{R}(S \leftarrow S') = \begin{pmatrix} -\widetilde{\cos}(\angle \boldsymbol{\rho}_2 \boldsymbol{\rho}) & -\cos(\theta)\sin(\phi_1) & \widetilde{\sin}(\angle \boldsymbol{\rho}_2 \boldsymbol{\rho}) \\ \cos(\theta_1)\sin(\phi_1) & \cos(\phi_1) & \sin(\theta_1)\sin(\phi_1) \\ -\sin(\angle \boldsymbol{\rho}_2 \boldsymbol{\rho}) & \sin(\theta)\sin(\phi_1) & \cos(\angle \boldsymbol{\rho}_2 \boldsymbol{\rho}) \end{pmatrix}, \tag{9}$$

where the different nonstandard symbolic terms have the following meanings:

$$\widetilde{\cos}(\angle \boldsymbol{\rho}_2\boldsymbol{\rho}) = \sin(\theta_1)\sin(\theta) - \cos(\theta_1)\cos(\theta)\cos(\phi_1),$$

$$\widetilde{\sin}(\angle \boldsymbol{\rho}_2\boldsymbol{\rho}) = \cos(\theta_1)\sin(\theta) + \sin(\theta_1)\cos(\theta)\cos(\phi_1),$$

$$\cos(\angle \boldsymbol{\rho}_2\boldsymbol{\rho}) = \cos(\theta_1)\cos(\theta) - \sin(\theta_1)\sin(\theta)\cos(\phi_1), \quad (10)$$

$$\sin(\angle \boldsymbol{\rho}_2\boldsymbol{\rho}) = \sin(\theta_1)\cos(\theta) + \cos(\theta_1)\sin(\theta)\cos(\phi_1).$$

Thus, using Eqs. (9) and (10), the CH$_5$ PES becomes fully determined by the 12 dynamic variables depicted in Fig. 1.

The coordinate system described above treats all the four H atoms (FABD) of the methane molecule equivalently. In fact, it makes no presumptions on the functionality of each atom and is of general applicability. This is in accordance with the fact that the JG-PES[15] is also symmetrical to exchange of the four H atoms in CH$_4$. The analytical functional form of the JG-PES, however, is nonsymmetrical with respect to the attacking hydrogen atom (atom E in Fig. 1). The fact that the CH$_5$ surface is not fully symmetrical in all of its five hydrogen atoms may cause a problem in this hydrogen-abstraction reaction. However, we believe this is not important in the present analysis, which is performed exclusively in the nonreactive AC at energies of up to 24 kcal mole^{-1}. This is because the barrier for E–F exchange is 35 kcal mole^{-1}[15] while the abstraction barrier is 10 kcal mole^{-1}.

To calculate ψ and χ [see Eqs. (5) and (7)], the determination of the full Hamiltonian of a hexa-atom molecule in body-fixed coordinates for a given total angular momentum $\mathbf{J}$ is required. For the present system, the optimal configuration is obtained by recursive application of the atom–diatom linking scheme.[40,43,44] Thus, the following expression for H under the stated coordinates and approximations may be worked out as

$$H = -\frac{\hbar^2}{2mr} \cdot \frac{\partial^2}{\partial r^2} r - \frac{\hbar^2}{2\mu_2\rho_2} \cdot \frac{\partial^2}{\partial \rho_2^2}\rho_2 - \frac{\hbar^2}{2\mu_1\rho_1} \cdot \frac{\partial^2}{\partial \rho_1^2}\rho_1$$
$$- \frac{\hbar^2}{2\mu\rho} \cdot \frac{\partial^2}{\partial \rho^2}\rho - \frac{\hbar^2}{2MR} \cdot \frac{\partial^2}{\partial R^2}R + \frac{\hbar^2}{2mr^2} \cdot \mathbf{j}^2 + \frac{\hbar^2}{2\mu_2\rho_2^2}$$
$$\cdot (\mathbf{j}_2 - \mathbf{j})^2 + \frac{\hbar^2}{2\mu_1\rho_1^2} \cdot (\mathbf{j}_1 - \mathbf{j}_2)^2 + \frac{\hbar^2}{2\mu\rho^2} \cdot (\mathbf{K} - \mathbf{j}_1)^2$$
$$+ \frac{\hbar^2}{2MR^2} \cdot (\mathbf{J} - \mathbf{K})^2 + U(r\rho_2\rho_1\rho R\theta_2\phi_2\theta_1\phi_1\theta\gamma\phi).$$
$$(11)$$

In Eq. (11), m, μ_2, and μ_1 are, respectively, the reduced masses of the DC (CH in the present research) stretch, the triatom BCD and the tetra-atom ABCD, while μ and M are those of the penta-atom FABCD (CH$_4$) and the atom–penta-atom EFABCD (HCH$_4$) systems. $\mathbf{j}$, $\mathbf{j}_2$, and $\mathbf{j}_1$ represent the bending angular momentum operators of the penta-atom (methane) molecule, while $\mathbf{K}$ is the total angular momentum operator of this last system. These rotational operators have the projections Ω, Ω_2, Ω_1, and Ω_K, respectively, in an arbitrary direction in the BF space. Because the quantum

mechanical numbers associated with the precession movements should be conserved, the following relation must hold:

$$\Omega_K = \Omega + \Omega_2 + \Omega_1. \quad (12)$$

A further explanation of the rotational dependence of the solutions of Eq. (11) is beyond the scope of this article.

C. Dynamics: Potentials and approximations

A fully quantum mechanical calculation involves 12 internal degrees of freedom and is not feasible using current computational facilities. Nevertheless, this work considers seven degrees of freedom (DOF). Five DOFs are treated in a fully dynamical fashion. The approaching angle γ is treated parametrically and the resulting probabilities are later averaged over.[45] Finally, the effect of out-of-plane precession is taken into account by averaging the potential around this angle:

$$\bar{U}(r\rho_2\rho_1\rho R\theta_2\phi_2\theta_1\phi_1\theta|\gamma)$$
$$= \frac{1}{2\pi}\int_0^{2\pi} U(r\rho_2\rho_1\rho R\theta_2\phi_2\theta_1\phi_1\theta\gamma\phi)d\phi. \quad (13)$$

[Note: because of the spherically symmetric properties of the methane (CH$_4$) molecule, the integration may be done more efficiently by integrating only over the interval $(0,\pi)$.]

The frozen degrees of freedom are treated within the IOSA, where bending angles and the rigid rotational motion of the CH$_4$ molecule are not allowed to change. This situation is depicted by an elastic wave function, where the rotational components are expressed by an explicit dependence on the angular momentum basis functions in the form $Y^{0,0}(\gamma,\phi) \times Y^{0,0}(\theta,0) \times Y^{0,0}(\theta_1,\phi_1) \times Y^{0,0}(\theta_2,\phi_2)$.

The potential of the asymptotic Hamiltonian H_λ, we denote as $V_\lambda = \bar{U} - V_r$, is written for this molecule as[45]

$$V_\lambda(r\rho_2\rho_1\rho R\theta_2\phi_2\theta_1\phi_1\theta|\gamma)$$
$$= v(r\rho_2\rho_1\rho\theta_2\phi_2\theta_1\phi_1\theta) + \bar{w}(R|\gamma). \quad (14)$$

v is the vibrational potential of the isolated (methane) penta-atom. $\bar{w}$ is also called the distortion potential and blocks the reaction path by forming a repulsive wall. Both of these potentials are constructed from U, the JG-PES, and are given by the following expressions:

$$v(r\rho_2\rho_1\rho\theta_2\phi_2\theta_1\phi_1\theta) = \lim_{R \to \infty} U(r\rho_2\rho_1\rho R\theta_2\phi_2\theta_1\phi_1\theta\gamma\phi),$$
$$(15)$$

$$\bar{w}(R|\gamma) = \bar{U}(r_e\rho_{2e}\rho_{1e}\rho_e R\theta_{2e}\phi_{2e}\theta_{1e}\phi_{1e}\theta_e|\gamma) - \text{const}. \quad (16)$$

Here U is the full hexa-atomic JG-PES expressed in terms of the reagent coordinates, $\bar{U}$ is the spherically averaged JG-PES defined in Eq. (13) and r_e, ρ_{2e}, ρ_{1e}, ρ_e, θ_{2e}, ϕ_{2e}, θ_{1e}, ϕ_{1e}, and θ_e are the equilibrium coordinates for the (methane) penta-atomic molecule, obtained by minimizing the JG-PES at large R. The const is selected in such a manner that $\lim_{R \to \infty} \bar{w}(R|\gamma) = 0$. These definitions ensure that V_r is localized to the reaction region.

TABLE I. Geometrical and energetic parameters characterizing the reaction $H+CH_4$ in the reagent asymptotic region, as deduced from the JG-PES (Ref. 15).

Parameter	Ref. 15	Ref. 23	Ref. 25	Present
Equilibrium distances (Å) Fig. 1				
r	1.094	1.094[a]		1.094
ρ_2				1.125
ρ_1				1.148
ρ_3				1.167
Equilibrium angles (deg) Fig. 1				
$180-\theta_2$	111.41[a]	107.45[a]		113.42
θ_1				108.93
θ	107.45[a]			106.00
ϕ_2				124.06
ϕ_1				64.469
Vibrational stretching frequency (see Ref. 15 for a definition of symbols)				
ν	0.3577			0.3496
ν_1				0.3666
ν_2	0.3784[3]			0.3686
ν_3				0.3718
Energetics (eV)				
ΔV_{min}	−0.121		−0.120	−0.120
ZPE (reagents)	1.182			0.740
ΔH_0	0.000 87		0.001	−0.017

[a]Refers to the CH_5 saddle point geometry.

III. THE REACTANTS

Since V_λ is a separable potential, the solution of Eq. (5) can be written as

$$\psi_{t_{i\lambda}}(r\rho_2\rho_1\rho R\theta_2\phi_2\theta_1\phi_1\theta\gamma|\nu\nu_1\nu_2\nu_3J)$$

$$=\frac{1}{r\rho_2\rho_1\rho R}\phi_\lambda(r\rho_2\rho_1\rho\theta_2\phi_2\theta_1\phi_1\theta\gamma|\nu\nu_1\nu_2\nu_3)$$

$$\times\zeta_\lambda(R|\nu\nu_1\nu_2\nu_3J), \qquad (17)$$

where ϕ_λ are the eigenfunctions [with vibrational eigenvalues $\epsilon(\nu\nu_1\nu_2\nu_3)$] of the equation[43]

$$\left[-\frac{\hbar^2}{2m}\frac{\partial^2}{\partial r^2}-\frac{\hbar^2}{2\mu_2}\frac{\partial^2}{\partial\rho_2^2}-\frac{\hbar^2}{2\mu_1}\frac{\partial^2}{\partial\rho_1^2}-\frac{\hbar^2}{2\mu}\frac{\partial^2}{\partial\rho^2}\right.$$

$$\left.+v(r\rho_2\rho_1\rho\theta_2\phi_2\theta_1\phi_1\theta)-\epsilon(\nu\nu_1\nu_2\nu_3)\right]$$

$$\times\phi_\lambda(r\rho_2\rho_1\rho\theta_2\phi_2\theta_1\phi_1\theta\gamma|\nu\nu_1\nu_2\nu_3)=0. \qquad (18)$$

Meanwhile $\zeta_\lambda(R|\gamma|\nu\nu_1\nu_2\nu_3J)$ are the solutions of the equation

$$\left[-\frac{\hbar^2}{2M}\cdot\frac{\partial^2}{\partial R^2}+\frac{\hbar^2}{2M}\frac{J(J+1)}{R^2}+\bar{w}(R|\gamma)\right.$$

$$\left.-\frac{\hbar^2}{2M}k^2(\nu\nu_1\nu_2\nu_3)\right]\zeta_\lambda(R|\gamma|\nu\nu_1\nu_2\nu_3J)=0. \qquad (19)$$

Here $k(\nu\nu_1\nu_2\nu_3)$ is the standard wave number defined by

$$k(\nu\nu_1\nu_2\nu_3)=\left[\frac{2M}{\hbar^2}(E-\epsilon(\nu\nu_1\nu_2\nu_3))\right]^{1/2}. \qquad (20)$$

Calculated asymptotic properties of the reagents $H+CH_4$ are shown in Table I and compared with previous published values wherever applicable. Our calculations assume that the bending angles are frozen in their equilibrium values, consistent with the IOSA assumption for the reactive scattering. This explains the small differences in the comparison. We first present equilibrium geometric parameters of distances and angles. Next, the vibrational frequencies are shown. Finally, energetic data is given. As discussed in the Introduction, the JG-PES does not treat all five hydrogen atoms equivalently. The abstracted hydrogen therefore has slightly different equilibrium angles and vibrational frequencies. Overall, the results presented in Table I show good agreement with results published by other groups. A further discussion of the implications concerning the reaction data will be given in Sec. V.

IV. DERIVATION OF THE PERTURBED WAVE FUNCTION

The perturbed wave function χ_λ is derived by solving Eq. (7) in the reagents AC. In order to accomplish this, we must use two negative imaginary potentials (NIPs). One NIP is placed in the far reagent asymptote (large R) to absorb the reflected (elastic and inelastic) wave. The other NIP is placed in the H_2+CH_3 channel (ρ) very close to its entrance and it absorbs the reactive flux. Both NIPs are of the Neuhauser–Baer linear ramp type,[39] their spatial extent was 1 Å, and their respective heights are 0.5 and 0.15 eV. At the considered energies, all other channels in the system are closed. The total imaginary potential is thus

$$V_I(r\rho_2\rho_1\rho R\gamma)\equiv-i[v_{1p}(\rho)+v_{IR}(R)]. \qquad (21)$$

We refer the reader to Sec. II B for a description of the coordinates and the various approximations used.

J. Chem. Phys., Vol. 117, No. 16, 22 October 2002

Five-D study of H+CH$_4$ reaction　　7619

Adding the two NIPs to the real potential U converts the scattering problem into a bound system problem. Consequently, χ can be expanded in terms of square integrable L^2 functions.[46–48] These are chosen as localized functions for the translational components and adiabatic basis sets for the four vibrational coordinates.[49,50] Thus, χ_λ, pertaining to a given angle γ may be written as[27] (here we start specifying explicitly the quantum numbers of the various wave functions)

$$\chi^J(r\rho_1\rho_2\rho R|t_f|\gamma t_i)$$

$$= \frac{1}{r\rho_1\rho_2\rho R} \sum_{nt} a^J_{nt}(t_f|\gamma t_i)g_n(R)f_{nt}(r\rho_1\rho_2\rho|\gamma), \quad (22)$$

where t_i and t_f indicate together collectively the quantum numbers identifying the initial and final state of the elastically colliding H+CH$_4$ system. In addition, $g_n(R)$ is the localized Gaussian function,[49,51]

$$g_n(R) = \left(\frac{\alpha}{\sigma\sqrt{\pi}}\right)^{1/2} \exp\left[-\frac{\alpha^2}{2}\left(\frac{R-R_n}{\sigma}\right)^2\right], \quad (23)$$

where $R_n (n=0,\ldots,N)$ are $N+1$ equidistant sectors along the translational axis R, α is a fitted dimensionless parameter, and σ is the grid spacing,

$$\sigma = R_n - R_{n-1}. \quad (24)$$

The choice of value for α is not crucial, as noted by Hamilton and Light,[51] who analyzed the behavior of this constant over the range (0.5–1.1). Moreover, Gilibert et al.,[29] who investigated the expansion of the translational wave function in terms of such localized Gaussian functions in a collinear scattering collision, found that a reasonable choice of the width of the Gaussian functions (σ/α) is given by

$$\frac{\sigma}{\alpha} = \frac{1}{\sqrt{2}k}, \quad (25)$$

where k is the same wave number defined in Eq. (20). From Eq. (25), it could be inferred that by assigning the greater values to α, fewer Gaussian functions will be required to meet the conditions of this equation. Nevertheless, from the influence of α on the numerical calculation of the phase shifts, a limit of $\alpha=1.5$ is advised.[29] To obtain well-converged IOSA results, the translational coordinate R extended from 1.55 to 4.5 Å and the grid spacing used was $\sigma=0.1$ Å.

As for $f_{nt}(r\rho_1\rho_2\rho|\gamma)$, it is an eigenfunction of the vibrational Hamiltonian H_{vib}:

$$(H_{\text{vib}} - \epsilon_t(R_n))f_{nt}(r\rho_1\rho_2\rho|\gamma)$$

$$= \left[-\frac{\hbar^2}{2m}\cdot\frac{\partial^2}{\partial r^2} - \frac{\hbar^2}{2\mu_2}\cdot\frac{\partial^2}{\partial\rho_2^2} - \frac{\hbar^2}{2\mu_1}\cdot\frac{\partial^2}{\partial\rho_1^2} - \frac{\hbar^2}{2\mu}\cdot\frac{\partial^2}{\partial\rho^2} \right.$$

$$\left. + \bar{U}(r\rho_2\rho_1\rho R|\theta_{2e}\phi_{2e}\theta_{1e}\phi_{1e}\theta_e|\gamma) - \epsilon_t(R_n)\cdot \right]$$

$$\times f_{nt}(r\rho_1\rho_2\rho|\gamma) = 0, \quad (26)$$

where $\epsilon_t(R_n)$ is the corresponding tth eigenvalue related to the eigenstates of Eq. (26). The four-dimensional functions $f_{nt}(r\rho_1\rho_2\rho|\gamma)$ are determined by the following scheme. For each of the independent variables (r,ρ_1,ρ_2,ρ) the other five variables are frozen at their equilibrium values and a one-dimensional vibrational Schrödinger equation is solved, to obtain N vibrational functions for that degree of freedom. For the variable ρ this Hamiltonian is non-Hermitian due to the presence of the NIP. Then, all possible fourfold products of these functions, regarded as a global basis, are used to construct a matrix representation of H_{vib}. The matrix is then diagonalized and its eigenvectors are used to construct $f_{nt}(r\rho_1\rho_2\rho|\gamma)$ as a linear combination of the fourfold global basis. This procedure must be solved at each grid point R_n. The number of global functions is determined so that a limiting energy of 2.5 eV is reached (see also a discussion in Ref. 48), thus this number may vary from one R grid point to another. Finally, the a^J_{nt} coefficients are obtained by solving Eq. (7) with the *ansatz* of Eq. (22). This is done by solving a linear set of algebraic equations using the (LU) decomposition method.[52] This set of equations must be solved separately for each value of γ.

Once the a^J_{nt} coefficients are known and replaced in Eq. (22) to compute χ, the scattering elements $S^J(t_f\leftarrow t_i)$ can be calculated by means of Eq. (4), under the form

$$S^J(t_f\leftarrow t_i) = \frac{1}{i\hbar}\left[\langle\psi^J_{t_f}|V|\psi^J_{t_i}\rangle + \sum_{nt} a^J_{nt}\langle\psi_{t_f}|V|g_nf_{nt}Y^{0,0}(\gamma,\phi) \right.$$

$$\left. \times Y^{0,0}(\theta,0)\times Y^{0,0}(\theta_1,\phi_1)\times Y^{0,0}(\theta_2,\phi_2)\rangle \right].$$

$$(27)$$

Formally, f_{nt} should include an explicit dependence on the same angular momentum basis function Y^{lm}. Since these spherical harmonic functions assume a constant value due to the IOSA concept, their inclusion in Eq. (22) is inconsequential because they will cancel when solving for χ in Eq. (7), irrespective of their value. Nevertheless, their role is important in the calculation of the scattering matrix elements and thus they are shown explicitly in Eq. (27).

The entire procedure outlined above is repeated for each value of J. Once the J-specific averaged reaction probabilities are obtained, the QM state-to-state reactive cross sections are calculated using

$$\sigma(t_f\leftarrow t_i) = \frac{\pi}{k^2(E_{\text{tr}})}\sum_J (2J+1)|S^J(t_f\leftarrow t_i)|^2, \quad (28)$$

where $k(E_{\text{tr}})$ is the standard number for the whole atom +penta-atom system, which is defined by $k^2(E_{\text{tr}}) = (2M/\hbar^2)E_{\text{tr}}$.

V. RESULTS AND DISCUSSION

Total reaction cross sections, as a function of the collision angle γ for several values of the translational energy in the range 0.3–0.7 eV, are given in Fig. 2. It is assumed that the methane molecule is in the ground vibrational state. Roughly speaking, for these energies, the aperture of the reaction is 25° or less, indicative of a substantial ''collinear''
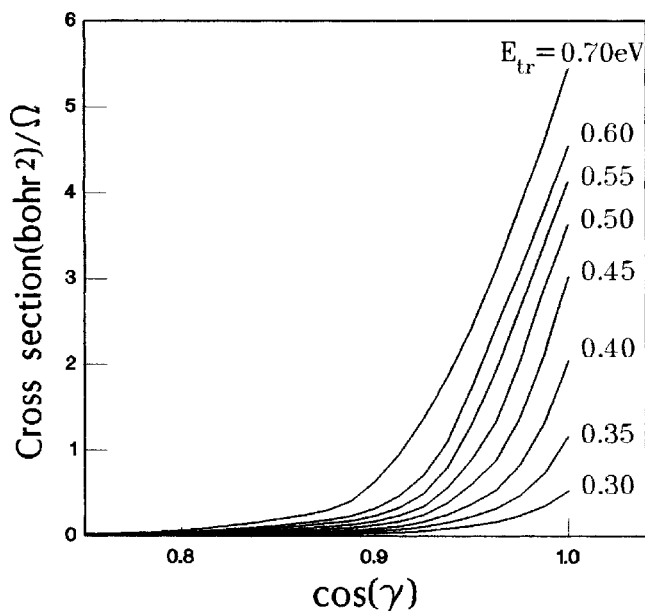
FIG. 2. The dependence of calculated integral cross sections for the reaction $H+CH_4 \rightarrow H_2+CH_3$ as a function of the incidence $\cos(\gamma)$. Curves shown were calculated for different values of E_{tr} ranging from 0.30 to 0.70 eV, as indicated in the figure.

FIG. 3. Opacity functions calculated as a function of the total angular momentum. Curves have been calculated for the same range of values of E_{tr}, as indicated in Fig. 2. (a) Standard absolute distribution. (b) Probability values weighted with the factor $(2J+1)$, showing the contribution of each J term to the integral cross section [see Eq. (28) in the text].

nature. A strong tunneling effect is observed as large cross sections at energies lower than the minimal reaction barrier of 0.473 eV.[15] The corresponding opacity functions are shown in Fig. 3 for the same values of the translational energy. The results are averaged over γ. The impact parameter can be deduced from these results and shows little sensitivity to E_{tr}, equal to $b=2.2$ Å. This value is somewhat larger than the value of $b=1.7$ Å found by classical calculations of Ref. 15 at similar energies. The optimal J value depends on the translational energy running from $J=10$ at $E_{tr}=0.3$ eV to $J=20$ at $E_{tr}=0.7$ eV.

A convenient way of perceiving the energetic characteristics of the PES consists of analyzing the energy dependence of the reaction probability at $J=0$ along a collinear trajectory ($\gamma=0$). Such results are shown in Fig. 4(a). Two striking features are evident. First, the threshold is at $E_{tr}=0.1$ eV, which is evidence for large tunneling effects, since the collinear barrier height is at 0.437 eV.[25] The second is the presence of resonance peaks in the reaction probability, centered at $E_{tr}=0.38$ eV and $E_{tr}=0.6$ eV. By changing the direction of collision γ, we depart from the saddle point geometry, the potential becomes more repulsive, and the reactivity diminishes appreciably. This is seen when we average over the collision angle γ [Fig. 4(b)]. The averaging also smears out the resonance structure. The consequence of this is that the average integral reaction probability looks much smoother and lower. The prediction of the SVRT model[23] is also shown in Fig. 4(b). These authors optimized the CH_4 geometry by assigning to the angles $(\theta, \theta_1, \theta_2)$ the transition state value of 107.45°, which corresponds to a barrier height about 0.48 eV. These calculations show a resonance peak at 0.53 eV. The two calculations show very different results that, in view of the different approximations, cannot be eas-
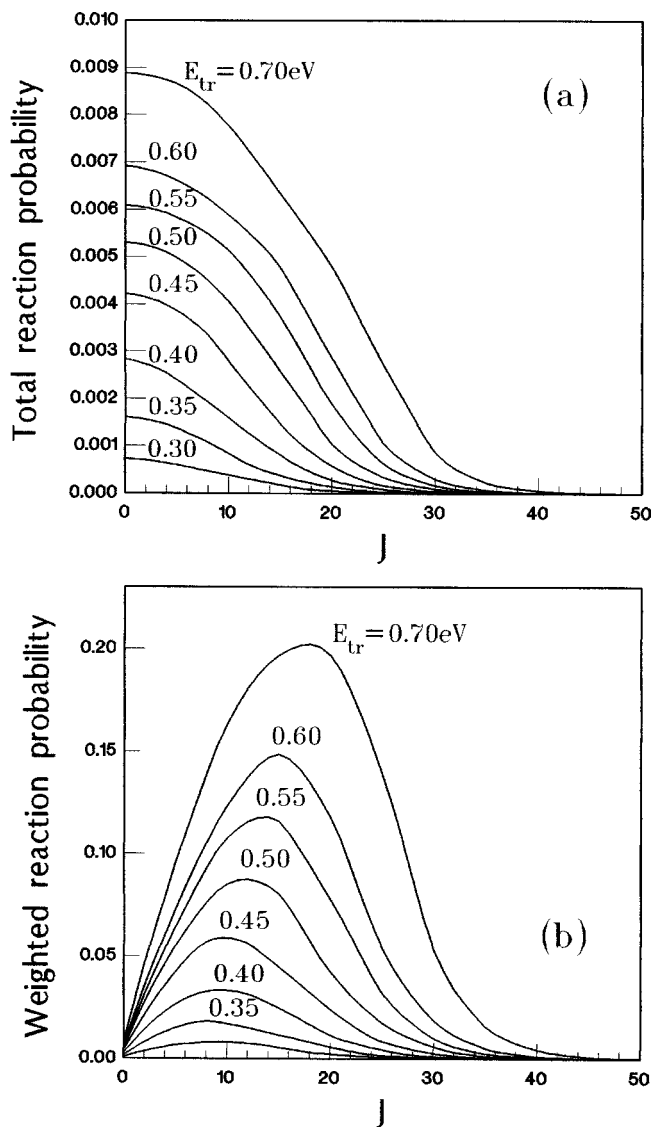
ily explained and remain an open question. Previous quantum dynamical calculations, although of limited dimensionality, also predict a collinear $J=0$ peak at low translational energies of 0.40[21] and 0.44 eV.[22]

One similarity, nevertheless, between the SVRT work and ours is the oscillatory structure of the reaction probability along the collinear direction as shown in curves (a) and (c) of Fig. 4. According to Ref. 23, this oscillatory structure is due to the broad dynamical resonances that exist in the $H+CH_4$ reaction. We observed, however, that this structure exists only close to the collinear orientation of the reaction axes, since this effect disappears after averaging all incident orientations. This can be seen in curve (b) of the same figure.

The calculated cross sections of Fig. 2 are averaged over the angle γ to yield the $H+CH_4$ reaction cross section as a function of translational energy. These are shown in Fig. 5(a). As can be seen from this figure, the quantum threshold
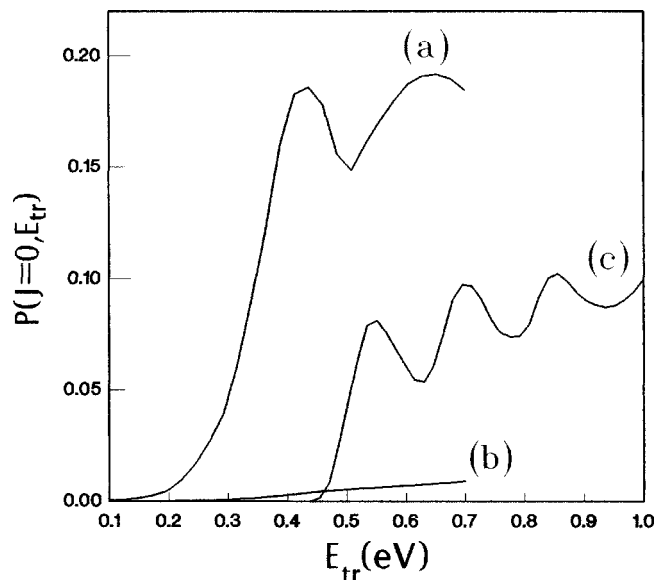
J. Chem. Phys., Vol. 117, No. 16, 22 October 2002

Five-D study of H+CH₄ reaction   7621

FIG. 4. Energy dependence of the reaction probability at the initial rotational ground state ($J=0$): (a) Along a collinear direction of the axes H–H–C(H$_3$); (b) the average over all orientations (γ,ϕ); (c) results taken from Ref. 23.

of the reaction is found at approximately 0.3 eV, which when compared to the *ab initio* barrier of 0.473 eV shows that tunneling effects are important. For comparison, results from Ref. 23 are also given in the same figure. Once again the threshold of the latter calculation is much higher, as discussed in connection with Fig. 4.

The thermal rate constants are calculated from the total cross section using the expression[53]

$$k=\left(\frac{1}{k_{\mathrm B}T}\right)^{3/2}\left(\frac{8}{\pi M}\right)^{1/2}\int_0^\infty E_T\sigma(E_T)e^{-E_T/k_{\mathrm B}T}\,dE_T,\quad (29)$$
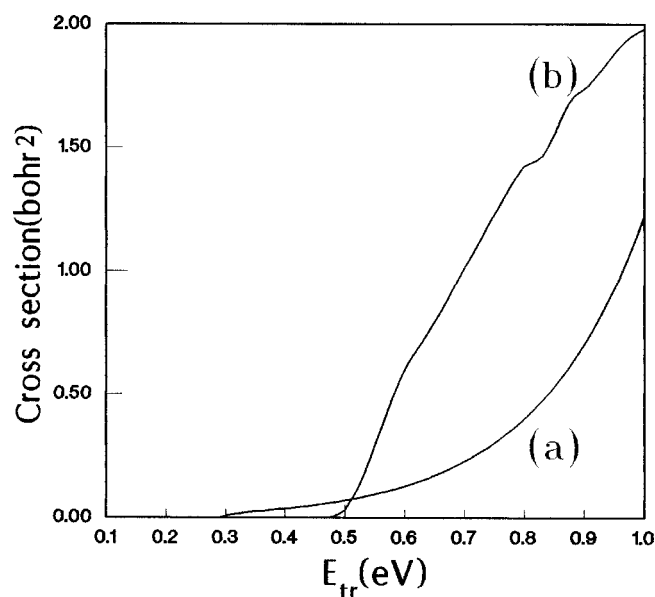

FIG. 5. The dependence of calculated integral cross sections for the title reaction as a function of the translational energy E_{tr}. (a) Present results; (b) results taken from Ref. 23.
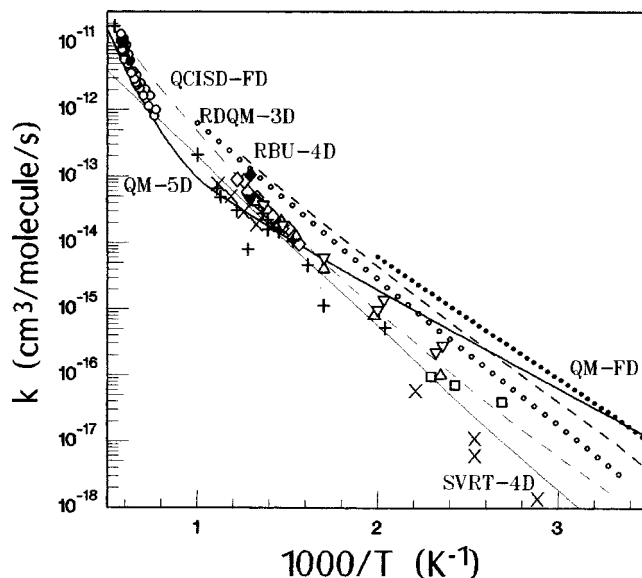

FIG. 6. Arrhenius plot of the rate constant k vs $1000K/T$ for the title reaction. (a) A full line (—) indicates the present results (QM-5D); (b) an open dotted line (○) represents reduced dimensionally QM (RDQM-3D) (Ref. 21) predictions; (c) a light line (—) SVRT (Ref. 23) ones; (d) a dotted line (●) represents full dimensional QM (QM-FD) calculations (Ref. 25); (e) the heavy dashed line (– – –) is the rotating bond umbrella (RBU-4D) model curve (from Ref. 22); (f) the light dashed line (– – –) represents QCISD predictions (from Ref. 24); (g) experimental points indicated as an open up triangle (△) (Ref. 4); dot (●) (Ref. 7); diamond (◇) (Ref. 11); solid diamond (◆) (Ref. 3); open dot (○) (Ref. 8); open square (□) (Ref. 1); full square (■) (Ref. 9); inverted triangle (▽) (Ref. 5); cross (+) (Ref. 10); (×) (Ref. 14).

where $k_{\mathrm B}$ is the Boltzmann gas constant and M the reduced mass of the atom+penta-atom system in Eq. (11). These computed rate constant values are presented in Fig. 6 as a solid line. The most striking feature is the strong departure from Arrhenius behavior showing up as a dependence of the slope on the temperature. The strong departure is evident already at relatively high temperatures of about 1000 K, in agreement with experimental results of Ref. 10.

For comparison purposes we also show in Fig. 6 rate constants obtained by different theoretical methods[21–25] as well as experimental data.[1–6,8–10,12–14] From an inspection of Fig. 6, it may be concluded at first sight that no theoretical calculation accurately describes the intensively researched experimental temperature rate constants of the title reaction in the 424–1600 K range. Referring to the closest curves to those of the experiment, we distinguish in Fig. 6 the variational transition-state results of Ref. 24 and the SVRT method.[23] The first is obtained using a different potential surface and thus cannot be directly compared to our calculations. The SVRT results use the JG-PES, but make different assumptions, in particular, using a smaller number of degrees of freedom. Their results yield a curve on the Arrhenius plot which agrees reasonably well with some experimental data in the 424–1000 K range. It fails, however, to describe the change of curvature at the 1000 K region. This issue, which can be easily explained as a quantum effect, is not new and has been discussed extensively in the past.[6,8,12] Our results,

however, provide a reasonable description of rate constants in the 600–2000 K range. At lower temperatures we compare well with the fully dimensional $J=0$ results of Ref. 25, which should be accurate at this regime. Thus, it is plausible that the discrepancy of the results is due to the quality of the potential energy surface and not to our model assumptions.

VI. SUMMARY AND CONCLUSIONS

A quantum mechanical approach was developed for treating abstraction processes such as the $H+CH_4 \rightarrow H_2+CH_3$ reaction. The general scheme is based on the arrangement decoupling imaginary potentials method.[36] The kinematics is described using generalized Jacobian coordinates and orbital angles. The full Hamiltonian, using the JG-PES, with its 12 internal degrees of freedom, is expressed using these coordinates. Treating the complete set of degrees of freedom is impractical at this stage, so we freeze, in their equilibrium position, the five internal bend angles of the methane molecule. This leaves seven active degrees of freedom, two angles and five radial coordinates to be considered. The studied process is thus that of a H atom attacking a rotating–stretching methane molecule. The rotations are not treated dynamically, instead IOSA is used and an averaging of the results over the several values of the incidence angle γ is made. The effect of the out-of-plane angle ϕ is taken approximately into account by averaging the potential over its values. Finally, the CS or j_z approximation was employed to decouple the total angular momentum $\mathbf{J}$ from internal rotational operators. This leads to a five-dimensional, fully quantum mechanical calculation. We proposed a method for carrying out this calculation and computing the integral reactive probabilities and cross sections of the $H+CH_4 \rightarrow H_2+CH_3$ reaction.

We first analyzed the reactants obtaining results that compare well to those of other groups. Concerning the reaction, we observed strong tunneling effects. The quantum translational energy threshold for the reaction was much lower than the potential energy barrier for this reaction. This also shows up as larger rate constants at lower temperatures, which are consistent with the full-dimensional $J=0$ calculations of Ref. 25. The present results predict a remarkable change in the linearity of the Arrhenius curve, in agreement with experimental results. This contrasts with previous reduced-dimensionally QM calculations.

Finally, it may be mentioned that important discrepancies were found here between the different quantum mechanical approaches. These could be attributed to differences in the methodologies applied, even though they all use quantum mechanical procedures. Thus, it is desirable to continue to improve the methodology so that higher dimensional treatments become possible. The present approach is general enough to be extended to high dimensions. In fact, we have considered all the radial degrees of freedom in this system and it now remains a computational challenge to include also the bending angles and rotations.

[1] M. R. Berlie and D. J. LeRoy, Can. J. Chem. **32**, 650 (1954).
[2] C. P. Fenimore and G. W. Jones, J. Phys. Chem. **65**, 2200 (1961).
[3] R. W. Walker, J. Chem. Soc., **A 1968**, 2391.
[4] M. Kurylo and R. B. Timmons, J. Chem. Phys. **50**, 5076 (1969).
[5] M. Kurylo, G. A. Holliden, and R. B. Timmons, J. Chem. Phys. **52**, 1773 (1970).
[6] T. C. Clark and J. E. Dove, Can. J. Chem. **51**, 2147 (1973).
[7] J. Peeters and G. Mahnen, in *Proceedings of the 14th International Symposium on Combustion* (Combustion Institute, Pittsburgh, 1973), p. 133.
[8] J. C. Biordi, J. F. Papp, and C. P. Lazzara, J. Chem. Phys. **61**, 741 (1974).
[9] J. C. Biordi, C. P. Lazzara, and J. F. Papp, in *Proceedings of the 15th International Symposium on Combustion* (Combustion Institute, Pittsburgh, 1975), p. 917.
[10] R. Shaw, J. Phys. Chem. Ref. Data **7**, 1179 (1978).
[11] A. Sepehrad, R. M. Marshall, and H. Purnell, J. Chem. Soc., Faraday Trans. **75**, 835 (1979).
[12] W. Tsang and R. F. Hampson, J. Phys. Chem. Ref. Data **15**, 1087 (1986).
[13] M. J. Rabinowitz, J. W. Sutherland, P. M. Patterson, and R. B. Klemm, J. Phys. Chem. **95**, 674 (1991).
[14] D. L. Baulch, C. J. Cobos, R. A. Cox *et al.*, J. Phys. Chem. Ref. Data **21**, 411 (1992).
[15] M. J. T. Jordan and R. G. Gilbert, J. Chem. Phys. **102**, 5669 (1995).
[16] T. Joseph, R. Steckler, and D. G. Truhlar, J. Chem. Phys. **87**, 7036 (1987).
[17] J. Espinosa-Garcia and J. C. Corchado, J. Phys. Chem. **100**, 16561 (1996).
[18] S. P. Walch, J. Chem. Phys. **72**, 4932 (1980).
[19] G. C. Schatz, S. P. Walch, and A. F. Wagner, J. Chem. Phys. **73**, 4536 (1980).
[20] E. Kraka, J. Gauss, and D. Cremer, J. Chem. Phys. **99**, 5306 (1993).
[21] T. Takayanagi, J. Chem. Phys. **104**, 2237 (1996).
[22] H.-G. Yu and G. Nyman, J. Chem. Phys. **111**, 3508 (1999).
[23] M. L. Wang, Y. Li, J. Z. H. Zhang, and D. H. Zhang, J. Chem. Phys. **113**, 1802 (2000).
[24] T. N. Truong, J. Chem. Phys. **100**, 8014 (1994).
[25] F. Huarte-Larrañaga and U. Manthe, J. Chem. Phys. **113**, 5115 (2000).
[26] J. M. Bowman, D. Wang, X. Wang, F. Huarte-Larrañaga, and U. Manthe, J. Chem. Phys. **114**, 9683 (2001).
[27] H. Szichman, M. Gilibert, M. González, X. Giménez, and A. Aguilar, J. Chem. Phys. **113**, 176 (2000).
[28] H. Szichman, M. Gilibert, M. González, X. Gimenez, and A. Aguilar, J. Chem. Phys. **114**, 9882 (2001).
[29] M. Gilibert, A. Baram, I. Last, H. Szichman, and M. Baer, J. Chem. Phys. **99**, 3503 (1993).
[30] H. Szichman, A. J. Verandas, and M. Baer, J. Chem. Phys. **102**, 3474 (1995).
[31] M. Baer, H. Szichman, E. Rosenman, S. Hochman-Kowal, and A. Perski, in *Springer Series in Chemical Physics, Vol. 61, Gas Phase Chemical Reaction Systems*, edited by J. Wolfrum, H.-R. Volpp, R. Rannacher, and J. Warnatz (Springer-Verlag, Heidelberg, 1996), p. 125.
[32] H. Szichman and M. Baer, J. Chem. Phys. **105**, 10380 (1996).
[33] H. Szichman, M. Baer, and H. Nakamura, J. Chem. Phys. **107**, 3521 (1997).
[34] H. Szichman, M. Baer, H.-R. Volpp, and J. Wolfrum, J. Phys. Chem. A **102**, 10455 (1998).
[35] M. Gilibert, X. Giménez, F. Huarte-Larrañaga, M. González, A. Aguilar, I. Last, and M. Baer, J. Chem. Phys. **110**, 6278 (1999).
[36] I. Last, D. Neuhauser, and M. Baer, J. Phys. Chem. **96**, 2017 (1992).
[37] R. T. Pack, J. Chem. Phys. **60**, 633 (1974).
[38] M. Arthurs and A. Dalgarno, Proc. R. Soc. London, Ser. A **256**, 540 (1960).
[39] D. Neuhauser and M. Baer, J. Chem. Phys. **90**, 4351 (1989).
[40] Z. Bačić and J. C. Light, Annu. Rev. Phys. Chem. **40**, 469 (1989).
[41] D. W. Jepsen and J. O. Hirschfelder, Proc. Natl. Acad. Sci. U.S.A. **45**, 249 (1959).
[42] M. E. Rose, *Elementary Theory of Angular Momentum* (Wiley, New York, 1957).
[43] J. Tennyson and B. T. Sutcliffe, J. Chem. Phys. **77**, 4061 (1982).

[44] H. Szichman and M. Baer, J. Chem. Phys. **101**, 2081 (1994).

[45] H. Szichman, M. Baer, and A. J. Varandas, J. Phys. Chem. A **101**, 8817 (1997).

[46] J. Z. H. Zhang, S. I. Chu, and W. H. Miller, J. Chem. Phys. **88**, 6233 (1988).

[47] M. Baer and H. Nakamura, J. Chem. Phys. **96**, 6565 (1992).

[48] I. Last, A. Baram, H. Szichman, and M. Baer, J. Phys. Chem. **97**, 7040 (1993).

[49] Z. Bačić and J. C. Light, J. Chem. Phys. **85**, 4594 (1986).

[50] J. Z. H. Zhang and W. H. Miller, J. Phys. Chem. **94**, 7785 (1990).

[51] I. P. Hamilton and J. C. Light, J. Chem. Phys. **84**, 306 (1986).

[52] W. H. Press, S. A. Teukolsky, W. T. Vetterling, and B. P. Flannery, *Numerical Recipes* (Cambridge University Press, Cambridge, MA, 1994), Chap. 2, p. 34.

[53] R. D. Levine and R. B. Bernstein, *Molecular Reaction Dynamics and Chemical Reactivity* (Oxford University Press, Oxford, 1987).